

Statistical physics of the solvated electron

G N Chuev

Contents

1. Introduction	149
2. Statistical theory of a solvated electron	150
2.1 Formalism of the statistical treatment; 2.2 Structural characteristics of a solvated electron; 2.3 Integral equations	
3. Description of the environment in terms of correlation functions	153
3.1 The Mayer cluster expansions method; 3.2 The direct correlation functions method	
4. Variational evaluation of the effective functional	154
4.1 Estimation by a trial action; 4.2 The Schrödinger equation and the effective potential for a solvated electron	
5. Specific features of the behaviour of a solvated electron in various media	155
5.1 Simple classical liquids; 5.2 Polar liquids; 5.3 Coulomb systems	
6. Many-particle quantum effects	160
6.1 Electron–electron correlations; 6.2 The problem of a dielectron	
7. Scope for the statistical approach	161
8. Conclusions	162
References	162

Abstract. Statistical models of an electron solvated in a classical liquid are reviewed. The analogy between the behaviour of a quantum particle and a polymer chain results in that statistical physics methods can be applied to the solvated electron problem. We have derived basic relations for thermodynamic and structural characteristics of the solvated electron. The free energy of the solvated electron and the effective electron–solvent potential as well as the electron–solvent correlation function are studied in detail. The calculated results are compared with experimental data and a quantum molecular dynamics simulation for simple, polar, and Coulomb liquids. We also outline many-particle quantum effects, such as electron–electron interactions and dielectron (bipolaron) formation. The potentialities and restrictions of the statistical method are also discussed.

1. Introduction

An actual problem of modern chemical physics is the study of a solvated electron, namely, an excess electron in a fluid, which does not make chemical bonds. The solvated electron is an object of intensive theoretical investigation and computer simulation (see, for example, reviews [1–5]). Such a mixed quantum-classical system is suitable to demonstrate the potential of various simulation methods such as quantum molecular dynamics, the path integral method, and a variety of combined schemes.

Numerous experimental techniques have been developed and extensive experimental evidence on the behaviour of the solvated electron in various media has been accumulated [6–13]. We wish to highlight two experimental facts, which seem the most impressive. The first is with the electron localization in a cavity formed due to interaction between the electron and ambient atoms [14, 15] (see also Ref. [16] considering two-dimensional analogs of such electron states). It is typical for nonpolar media and occurs in liquid helium. The second example is concerned with polar liquids, where the solvated electron is considered as an anion of characteristic radius about 3 Å, surrounded by a solvent shell of complicated structure [17–19].

Present-day theoretical approaches are based on the assumption that the behaviour of a solvated electron is similar to that of a closed polymer chain. Strictly speaking, the problem of a quantum particle in a liquid can be reduced to that of calculating the configuration of the isomorphic ring chain [20].

Figure 1 shows schematically the configuration of such polymer in a solvent. Full circles represent the electron density distribution, while the open circles correspond to liquid particles. The above-cited examples are the limiting cases of the polymer chain behaviour. Cavity formation takes place when the polymer resides in a poor solvent and a polymer globule arises (Fig. 2), while the complex solvate structure is generated when the attractive forces between polymer units and solvent particles prevails (see Fig. 3 depicting the simulation data for an electron solvated in water [21]).

The analogy between the problems enables one to use various numerical procedures [22–31] and methods developed in the theory of equilibrium liquids [32]. The statistical approach appears extremely efficient for calculating a variety of characteristics of a solvated electron [33–58]. Its accuracy is highly competitive with that obtainable in simulation by the

G N Chuev Institute for Mathematical Problems of Biology, Russian Academy of Sciences, 142292 Pushchino, Moscow Region, Russia
Tel. (7-0967) 73 25 16. Fax (7-0967) 73 24 08
E-mail: chu@impb.serpukhov.su

Received 9 April 1998, revised 28 July 1998
Uspekhi Fizicheskikh Nauk 169 (2) 155–170 (1999)
Translated by G N Chuev; edited by A Radzig

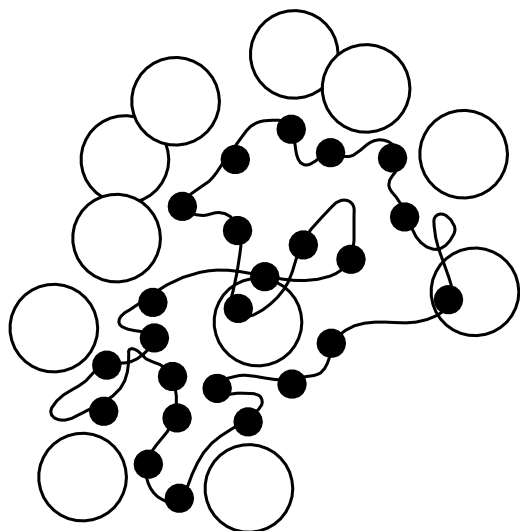


Figure 1. Schematic representation of a solvated electron as a closed polymer chain. Full circles conform to the electron density distribution, while the open circles correspond to liquid particles.

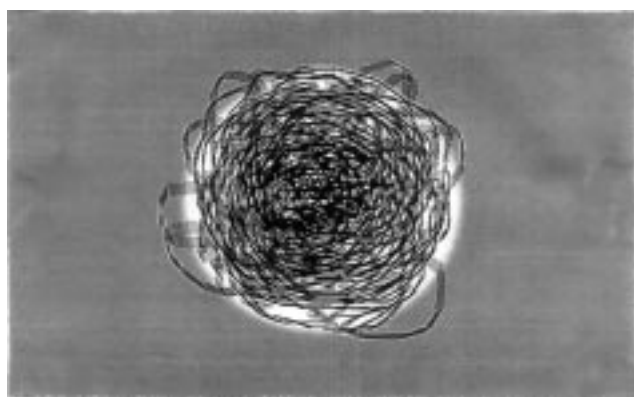


Figure 2. A closed polymer chain behaves similarly to an electron solvated in liquid helium, forming a cavity.

Monte Carlo or quantum molecular dynamics methods. On the other hand, using this approach, we can describe the electron behaviour on a microscopic level and derive nearly analytical dependences of the structural and energetic characteristics of the solvated electron on the macro- and microscopic parameters of the liquid, such as density, temperature, pressure, size and charge of solvent particles, etc.

This work provides a review of statistical models of a solvated electron, outlining the main methods and results obtained by this approach. Our aim is to show that the solvated electron serves as a new and extremely interesting object for which statistical physics methods are suited. These methods enable us to understand the behaviour of a quantum particle in a liquid, considering the liquid as a spatially disordered medium. Section 2 is devoted to the statistical theory of the solvated electron. There we present the formalism of the statistical approach and give the basic relations for the thermodynamic and structural characteristics of the solvated electron. The similarity of the problems of the solvated electron and polyatomic molecule allows us to use the method of integral equations, described in Section 2.3,

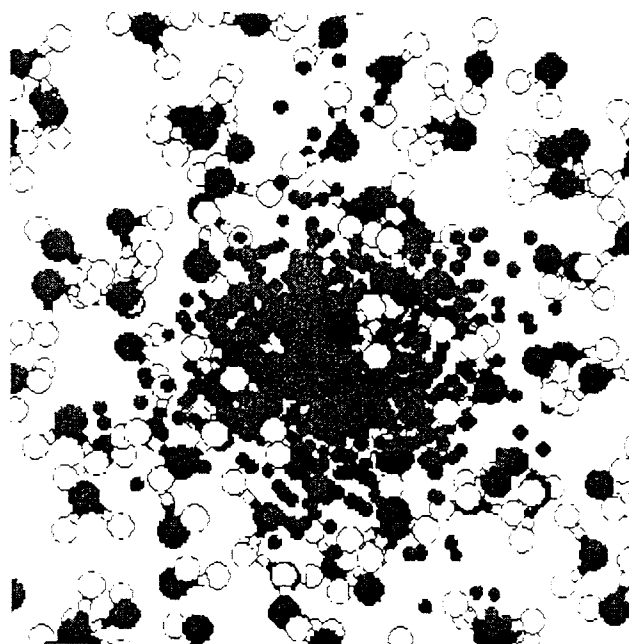


Figure 3. A closed polymer chain generates a complex solvate structure. The Monte-Carlo simulation data for an electron hydrated in water [21]. The symbols are the same as in Fig. 1; the bonds between polymer units are not shown.

to investigate the solvated electron behaviour. In Section 3 we consider two main approaches: Mayer cluster expansions and the method of direct correlation functions, which enable us to provide a concise description of a classical liquid and reduce the problem to the evaluation of a path integral. In Section 4 we submit a variational evaluation of the path integral and obtain general relations for the free energy and the effective potential of a solvated electron. In Section 5 the results of calculations with the use of the statistical models are compared with experimental data and the theoretical expectations based on quantum molecular dynamics for an electron solvated in nonpolar, polarizable, polar, and Coulomb liquids. Section 6 presents the potentialities of the method related to the consideration of many-body quantum effects such as electron–electron interactions and the formation of bipolaron (dielectron) states. Other potentialities of the method as well as its restrictions are discussed in Section 7.

Expounding the theory we tried to avoid rigorous mathematical derivations, restricting ourselves to the basic relations.

2. Statistical theory of a solvated electron

2.1 Formalism of the statistical treatment

Solvent atoms interacting with a solvated electron set up a complicated potential field for the electron. A detailed consideration of this field is an extremely intricate problem. However, there is a large parameter N of the theory, i.e. the number of interacting solvent atoms, which allows us to treat the field as random, use self-averaging, and reveal the dependence of the solvated electron behaviour on the averaged parameters of the liquid. In this statistical approach the problem is reduced to the calculation of the partition function. For an electron solvated in a classical

liquid the partition function Z can be written in terms of a configuration integral depending on the configuration of classical particles $\mathbf{R}_1, \mathbf{R}_2 \dots = \mathbf{R}^{\{N\}}$, and a path integral taken over the electron path $\mathbf{r}(\tau)$:

$$Z \propto \int D[\mathbf{r}(\tau)] \int d\mathbf{R}^{\{N\}} \exp \left[-\beta U_{ss}(\mathbf{R}^{\{N\}}) - \int_0^\beta d\tau \left[\frac{1}{2} \dot{\mathbf{r}}^2(\tau) + \sum_i u(\mathbf{r}(\tau) - \mathbf{R}_i) \right] \right]. \quad (1)$$

Here U_{ss} is the interaction potential between the particles of the liquid, $u(\mathbf{r} - \mathbf{R}_i)$ is the pairwise interaction potential between the electron and a solvent particle, and \mathbf{R}_i is the coordinate of the i th solvent particle. In the above relation $k_B T = 1/\beta$ is the temperature (we use the system of units for which $\hbar = 1, m_e = 1$), while the symbols $\mathbf{D}[\mathbf{r}(\tau)]$ stand for

$$\mathbf{D}[\mathbf{r}(\tau)] \propto \lim_{n \rightarrow \infty} \int_{\mathbf{r}_1 = \mathbf{r}}^{\mathbf{r}_n = \mathbf{r}'} \dots \int d\mathbf{r}_1 d\mathbf{r}_2 \dots d\mathbf{r}_n.$$

Let us consider a closed polymer chain consisting of n units. Assume that the size of the units is small ($l \rightarrow 0$), and their number is large ($n \rightarrow \infty$), while $\beta = nl^2$ takes finite values. In what follows we use the functional variable $\mathbf{v} = \tau l^2$ instead of τ . Then relation (1), correct to the notation, will describe the partition function of the polymer chain consisting of n units, with the interaction potential equal to $l^{-2}u(\mathbf{v} - \mathbf{R})$ [20, 59]. The representation of the partition function of polymer chain as a path integral is based on a deep analogy between quantum mechanics and Brownian motion, which was repeatedly pointed out earlier [60, 61].

If we know the partition function $Z(\beta)$ or the corresponding density matrix $\varrho(\mathbf{r}, \mathbf{r}, \beta)$ ($Z = \int \varrho(\mathbf{r}, \mathbf{r}, \beta) d\mathbf{r}$), we can directly calculate various averages

$$\langle A \rangle \propto \iint \varrho(\mathbf{r}, \mathbf{r}', \beta) A(\mathbf{r}, \mathbf{r}') d\mathbf{r} d\mathbf{r}'$$

characterizing the electron state: its mean radius squared $\langle R^2 \rangle$, the average interaction potential $\langle u(r) \rangle$ between the electron and a particle, the influence of weak external fields, etc.

One can also calculate the thermodynamic properties of the electron state, such as the free energy F , entropy Γ_{ent} , and average energy E :

$$\beta F = -\ln Z, \quad \Gamma_{\text{ent}} = \beta^2 \frac{\partial F}{\partial \beta}, \quad E = F + \frac{1}{\beta} \Gamma_{\text{ent}}. \quad (2)$$

Thus, the problem of an electron solvated in a classical liquid is reduced to calculations of a multiple integral (1). In present-day numerical calculations $N \sim 300$, while the relevant polymer chain contains $n \sim 300$ units [24], i.e. the integral multiplicity is huge. Hence, the main problem of the theoretical treatment of expression (1) is to reduce the integral multiplicity, preserving all the interesting physical properties of the system under consideration. In some cases, the possibility of such a concise description is provided by a special choice of potentials $U_{ss}(r)$ and $u(r)$, allowing one to integrate relation (1) analytically for some degrees of freedom. In other cases, it can be realized due to the low dimensionality of the space.

In our conditions we can divide the problem into several stages.

In the first stage, we should provide a concise description for liquid. For this purpose, the influence of the electron on the environment is considered as an external field $\langle u \rangle$, and one evaluates the configuration integral in (1) using the statistical physics methods based on various group expansions (see, for example, Refs [62, 63]). As a result, we derive a path integral with an effective influence functional $F_{\text{eff}}(\mathbf{r}(\tau))$ depending on the thermodynamic and structural parameters of the liquid. Some examples of such transformations are presented in Section 3.

The second stage deals with the variational evaluation of the path integral obtained. The evaluation implies solution of nonlinear equations, resulting in a self-consistent calculation of the dependence of the electron density distribution on the density ρ , temperature T and other parameters of the liquid. The scheme of this evaluation is outlined in Section 4.

At the final stage, using the dependences obtained, we calculate the parameters of the solvated electron which can be examined experimentally: the electron mobility $\mu(\rho, T, \dots)$, the absorption coefficient $k(\omega, \rho, T, \dots)$, susceptibility, etc. Some examples of such calculations and a comparison with the experimental data are given in Section 5. The above quantities are expressed in terms of the solvated electron structural characteristics, which are responsible for the electron behaviour in space and time and for structural changes in the solvent caused by the electron.

2.2 Structural characteristics of a solvated electron

To determine the solvated electron behaviour, we should average the density matrix of the whole system $\varrho(\mathbf{R}^{\{N\}}, \mathbf{r}, \mathbf{r})$ over classical configurations $\mathbf{R}^{\{N\}}$ and calculate the wave function for the electron ground state $\varphi(r)$: $\langle \varrho(\mathbf{R}^{\{N\}}, \mathbf{r}, \mathbf{r}) \rangle_{\mathbf{R}^{\{N\}}} = \varrho_0(\mathbf{r}, \mathbf{r}) \propto \varphi^2(\mathbf{r})$. For simple estimates it is sufficient to use the Gaussian wave function

$$\varphi(r) = \left(\frac{2\alpha}{\pi} \right)^{3/2} \exp[-\alpha^2 r^2]. \quad (3)$$

The wave function $\varphi(\mathbf{r})$ is applied to obtain the average parameters $\langle A \rangle \equiv \int A(\mathbf{r}) \varphi^2(\mathbf{r}) d\mathbf{r}$.

Another important structural characteristic of the solvated electron is the electron-solvent binary distribution function $g_{\text{es}}(\mathbf{r})$ which describes the probability of a solvent particle occurring at a distance \mathbf{r} from the centre of the electron localization:

$$g_{\text{es}}(\mathbf{r}) = -\frac{\delta \ln Z}{\delta \langle \beta u(\mathbf{r}) \rangle}, \quad (4)$$

and coincides with the definition of a binary distribution function [63] for a classical particle with the potential $\langle u \rangle = \int u(\mathbf{r}) \varphi^2(\mathbf{r}) d\mathbf{r}$. In the general case $g_{\text{es}}(r \rightarrow \infty) = 1$, but $g_{\text{es}}(r \rightarrow 0) \neq 0$, which is due to the quantum behaviour of the solvated electron. As for a classical liquid we can introduce the total electron-solvent correlation function

$$h_{\text{es}}(\mathbf{r}) = 1 - g_{\text{es}}(\mathbf{r}).$$

The function $g_{\text{es}}(\mathbf{r})$ determines the behaviour of the solvate structure around the electron, which depends on the type of interactions between the electron and the solvent particles. Using $g_{\text{es}}(\mathbf{r})$, one can also calculate the coordination number [44] and other characteristics of the solvate structure. The quantitative measure of predominance of repulsive or

attractive forces is ΔN , which defines a change in the average number of solvent particles bound to the electron, as compared to uniform liquid density:

$$\Delta N = \rho \int [g_{es}(\mathbf{r}) - 1] d\mathbf{r}. \quad (5)$$

At $\Delta N < 0$, repulsive forces prevail and a cavity of typical size α^{-1} is formed. When $\Delta N > 0$, attractive forces are dominant and a cluster arises. Figures 4 and 5 show these two types of behaviour of $g_{es}(r)$. Figure 4 demonstrates the electron–solvent binary function for different polarizabilities of solvent atoms [58]. The curves 1 ($\mu = 23a_0^3$) and 2 ($\mu = 15a_0^3$) (a_0 is the Bohr radius) correspond to cluster formation, and the curve 3 ($\mu = 0$) represents bubble formation.

The other limiting case is illustrated in Fig. 5 where the binary radial distribution function $g_{eK^+}(r)$ in molten KCl is depicted [44]. As is seen, a complex solvate structure arises near the centre of the electron localization.

Among the structural characteristics of the solvated electron the quantity $R^2(t) = \langle |\mathbf{r}(t) - \mathbf{r}(0)|^2 \rangle$, i.e. the mean square of displacement, plays a peculiar role. This quantity

describes the response of the system to a weak external perturbation; it determines the rates of various relaxation processes or corresponding kinetic coefficients (see Section 5). Applying the fluctuation-dissipative theorem, we can relate it to the generalized susceptibility [45]. The mean square of displacement characterizes not only the ground electron state, but also the excited states. A rough estimate of the lowest excitation energy E_1 and the absorption maximum $\omega_{\max} = E_1 - E_0$ can be found from the approximation

$$R^2(t) = R_0^2 [1 - \exp(-\omega_{\max} t)]^2, \quad 0 \leq t \leq \frac{\beta}{2}. \quad (6)$$

The quantity R_0^2 is related to the parameter α : $R_0^2 = (3/4)\alpha^{-2}$, and presents the mean radius squared of the solvated electron. In the general case, $R^2(t)$ is time-dependent, therefore to calculate it we should carefully investigate the asymptotic behaviour of the electron as a function of a complex variable $\tau + it$ and use relevant methods of analytic continuation [36]. For the free electron $R^2(t)$ is calculated analytically: $R_{\text{free}}^2(\tau) = 3\tau(1 - \tau/\beta)$. The typical behaviour of $R(\tau)$ is shown in Fig. 6. The solid line corresponds to the free electron, and the dashed one to a localized electron state.

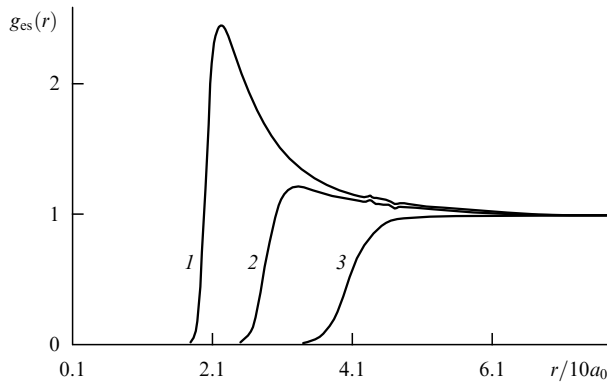


Figure 4. Electron–solvent binary function for different polarizabilities of solvent atoms [58]. Curve 1 applies to $\mu = 23a_0^3$, 2 — $\mu = 15a_0^3$, and 3 — $\mu = 0$.

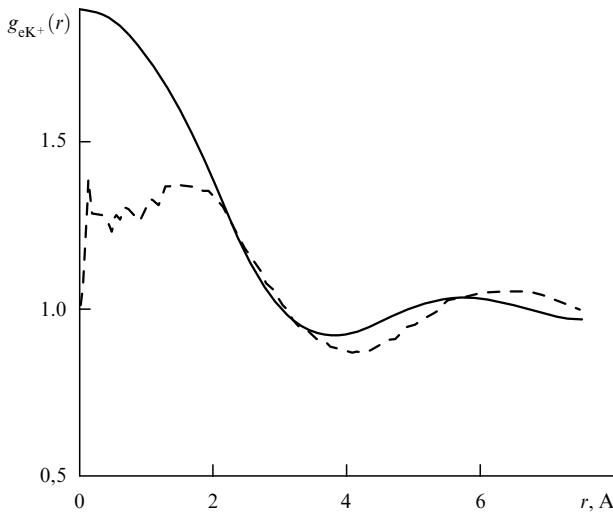


Figure 5. Binary radial distribution function $g_{eK^+}(r)$ in molten KCl [44] at $T = 1000$ K; the dashed line corresponds to the path-integral simulation data [22].

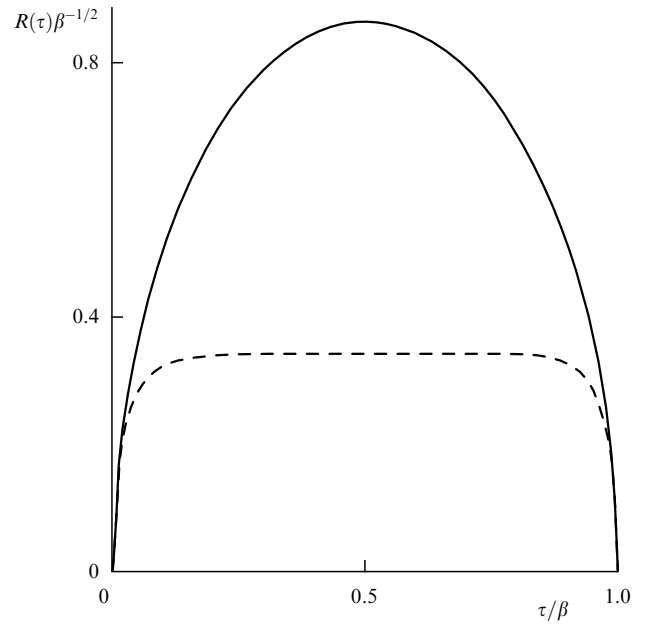


Figure 6. Dependence $R(\tau)\beta^{-1/2}$. The solid line corresponds to the free electron, and the dashed one to a localized electron state.

By analogy with the polymer chain we can also introduce a self-pair electron correlation function [33]

$$\omega_e(|\mathbf{r} - \mathbf{r}'|, \tau - \tau') = \langle \delta[\mathbf{r} - \mathbf{r}' - \mathbf{r}(\tau) + \mathbf{r}'(\tau')] \rangle. \quad (7)$$

This describes the probability of two chain units with subscripts τ and τ' occurring at a distance $|\mathbf{r} - \mathbf{r}'|$. The Fourier transform of the correlation function is defined by the mean square of displacement: $\omega_e(k, \tau) = \exp[-k^2 R^2(\tau)/6]$. The Fourier transform of the average self-pair electron correlation function can be expressed in terms of the wave function of the electron ground state:

$$\omega_e^0(\mathbf{k}) = \beta^{-1} \int_0^\beta d\tau \omega_e(\mathbf{k}, \tau) = \varphi^2(\mathbf{k}). \quad (8)$$

The functions $\varphi(\mathbf{r})$, $g_{\text{es}}(\mathbf{r})$, $R^2(t)$, and $\omega_e(k, \tau)$ are related to each other. The solvated electron induces a mean field $\langle u(\mathbf{r}) \rangle$ depending on the electron density distribution determined by $\varphi(\mathbf{r})$ or $\omega_e^0(\mathbf{r})$. This results in a rearrangement of the solvent particles and an effective density ρg_{es} . In turn, the mean field $\langle u(\mathbf{r}) \rangle$ depends self-consistently on g_{es} . Thus, the problem reduces to calculation of the functional dependence $g_{\text{es}}(\langle u(\mathbf{r}) \rangle)$.

2.3 Integral equations

In practice it is rather difficult to reveal the functional dependence $g_{\text{es}}(\langle u(\mathbf{r}) \rangle)$. In some cases it is more convenient to lean upon integral equations, for example, the Ornstein–Zernike equation for a solvated electron [33]:

$$h_{\text{es}}(\mathbf{r}) = \langle c_{\text{es}}(\mathbf{r}) \rangle + \rho \int \langle c_{\text{es}}(\mathbf{r} - \mathbf{r}') \rangle h_{\text{ss}}(\mathbf{r}') d\mathbf{r}' \\ = \langle c_{\text{es}} \rangle + \rho \langle c_{\text{es}} \rangle * h_{\text{ss}}. \quad (9)$$

Here the symbol ‘*’ denotes convolution integration, while $h_{\text{ss}}(\mathbf{r})$ is the total correlation function for uniform liquid. This equation links h_{es} and the direct correlation function $\langle c_{\text{es}} \rangle$ responsible for the direct effect of a solvent particle on the electron density distribution. The Ornstein–Zernike equation is exact, but requires an additional closure determining the asymptotes $h_{\text{es}}(r \rightarrow 0)$ and $\langle c_{\text{es}}(r \rightarrow \infty) \rangle$. Two most frequently used closures are the hypernetted chain closure (HNC) applied to Coulomb systems, and the Percus–Yevick (PY) approximation ($h_{\text{es}} = -1$, $r < r_0$, $\langle c_{\text{es}} \rangle = 0$, $r > r_0$). The latter is employed for liquids with a short-range repulsion potential.

At first glance it would seem that we have complicated the problem. Rather than straightforwardly seek the dependence $g_{\text{es}}(\langle u(\mathbf{r}) \rangle)$, we introduced the additional function $c_{\text{es}}(r)$ and used some additional approximations. However it turns out that in the equilibrium liquid theory there are well devised closure schemes as well as numerical and analytical methods for solving the related equations (9) (see, for example, Ref. [64]).

The physical meaning of the quantity $\langle c_{\text{es}}(r) \rangle$ can be revealed if the field $\langle u(\mathbf{r}) \rangle$ is considered as external. Then it can be defined as the direct correlation function for the liquid in this field [65, 66]:

$$g_{\text{es}}(r) = \exp[-\beta \langle u(r) \rangle + \langle c_{\text{es}}(r) \rangle]. \quad (10)$$

Certainly, the evaluation of dependence (10) as well as $g_{\text{es}}(\langle u(\mathbf{r}) \rangle)$ is rather complicated in most cases, therefore, sometimes it is to more advantage to solve Eqn (9) employing various approximations for closure.

Another useful relation is the Kirkwood integral equation [50]

$$\ln g_{\text{es}}(\mathbf{r}) = -\beta \langle u(\mathbf{r}) \rangle \\ - \rho \beta \int_0^1 d\zeta \int d\mathbf{r}' \langle u(\mathbf{r}') \rangle g_{\text{es}}(\mathbf{r}', \zeta) h_{\text{ss}}(\mathbf{r} - \mathbf{r}'). \quad (11)$$

Here ζ is the coupling coefficient corresponding to the introduction of an additional quantum particle (an excess electron), while $g_{\text{es}}(\mathbf{r}) \equiv g_{\text{es}}(\mathbf{r}, \zeta = 1)$. This equation determines in a self-consistent way the dependence $g_{\text{es}}(\langle u(\mathbf{r}) \rangle)$. However, some additional suggestions about $g_{\text{es}}(\mathbf{r})$, depending on the coupling coefficient ζ , are required to solve it.

3. Description of the environment in terms of correlation functions

The first step in reducing the multiplicity of integral (1) consists in providing a concise description of the environment in terms of correlation functions. Here we describe two main ways to derive the effective electron functional, i.e. the one based on the group expansions, and the method leaning upon integral equations of type (10).

3.1 The Mayer cluster expansions method

Using the Mayer cluster expansions method [67], the configuration integral in Eqn (1) can be written via solvent density correlation functions. Then, the partition function (1) is transformed into a path integral with an effective functional F_{eff} depending on these correlation functions [48, 52, 53]. Let us introduce the generalized Mayer function $f(r)$ of a quantum particle, defined as

$$f(\mathbf{r} - \mathbf{R}) = \exp \left[- \int_0^\beta u(\mathbf{r}(\tau) - \mathbf{R}) d\tau \right] - 1. \quad (12)$$

Although this expression does not simplify the calculation of the configuration integral, it enables us to use further approximations. For example, the irreducible density correlation functions of order higher than three are often ignored for a liquid or a dense gas. Then, integral (1) is expressed [53] as

$$Z \propto \int D[\mathbf{r}] \exp[-\beta F_{\text{eff}}(\mathbf{r})] \\ = \int D[\mathbf{r}] \exp \left[- \int_0^\beta d\tau \frac{1}{2} \dot{\mathbf{r}}^2(\tau) + f * \rho + \frac{1}{2} f * \chi_2 * f \right]. \quad (13)$$

In this relation the correlation function $\chi_2(\mathbf{R}) = \rho^2 h_{\text{ss}}(\mathbf{R})$ can be found either by using analytical theories or employing molecular simulation. For simple liquids, the information on the function can be obtained experimentally [63]. We can also include solvent density correlations of a higher order in the effective functional, when needed.

In effect, the method under consideration reduces the problem to the evaluation of the averages $\langle f \rangle$ and $\langle f * \chi_2 * f \rangle$. The evaluation can be consistently carried out if the short-range repulsion potential is dominant and $\langle f \rangle$ varies from -1 to 0 . The method is adequate for simple classical liquids (see Section 5)

3.2 The direct correlation functions method

The other method leans upon the direct correlation function $c_{\text{es}}(r)$ and was first implemented in the reference interaction site model (RISM-polaron theory) [33–47, 51]. In this approach use is made of the effective influence functional

$$\beta F_{\text{eff}}^{\text{RISM}} = \int_0^\beta \left[\frac{1}{2} \dot{\mathbf{r}}^2(\tau) - \frac{1}{\beta} c_{\text{es}}(\mathbf{r}(\tau) - \mathbf{R}) * \rho \right] d\tau \\ - \frac{1}{2\beta^2} \int_0^\beta \int_0^\beta c_{\text{es}}(\mathbf{r}(\tau) - \mathbf{R}) * \tilde{\chi}_2 * c_{\text{es}}(\mathbf{r}(\tau') - \mathbf{R}') d\tau d\tau', \quad (14)$$

where $\tilde{\chi}_2(\mathbf{r}) = \rho^2 \delta(\mathbf{r}) + \rho^2 h_{\text{ss}}(\mathbf{r})$. In contrast to Eqn (13), a rigorous derivation of Eqn (14) is lacking. The choice of effective functional (14) is motivated by the assumption that the solvent is characterized by the Gaussian density distribution $P_G[\rho(\mathbf{r})]$ for which the function $c_{\text{es}}(\mathbf{r}(\tau) - \mathbf{R})$ determines the coupling between the electron and a solvent particle [33]. When the potential $\beta u(\mathbf{r}) \ll 1$ is weak, relation (14) coincides with (13) to an accuracy of terms quadratic in β .

In turn, the average direct correlation function $\langle c_{\text{es}}(r) \rangle$ and $h_{\text{es}}(r)$ are related, as in the RISM theory [32], by the integral equation

$$\rho h_{\text{es}}(\mathbf{r}) = \int d\mathbf{r}_1 \int d\mathbf{r}_2 \langle c_{\text{es}}(|\mathbf{r}_1 - \mathbf{r}_2|) \rangle \omega_e^0(|\mathbf{r} - \mathbf{r}_1|) \tilde{\chi}_2(\mathbf{r}_2). \quad (15)$$

An essential feature of Eqn (15) is that an additional closure of PY or HNC type is required to solve it, but the explicit form of the dependence $g_{\text{es}}(\langle u(r) \rangle)$ is not necessary. Notice that the functional involving direct correlation functions is quadratic in β , whereas the influence functional (13) is not. In this sense, functional (14) is similar to the polaron effective action [80], and hence the methods used for evaluating the polaron action can be applied to this case too.

Formulae (13) and (14) express the effective interaction between the environment and the solvated electron in terms of solvent density correlation functions. Therefore the potential between the electron and a solvent particle is a preassigned function, while the solvent density is a random quantity responsible for state fluctuations in the system. In some problems of physics of disordered systems [68–70], the effective electron–medium interaction potential is treated as a random quantity, and various approximations of this interaction are used. In the relationships under consideration, we used correlation functions of a uniform liquid and functions which can be found independently from the equilibrium liquid theory. The pairwise electron–atom potential can also be obtained independently from the quantum-chemical calculations [71–73].

Besides, there are a number of statistical models of a solvated electron, where some parameters of the effective potential are taken as statistical quantities. To illustrate, these are the number of molecules in the first coordination shell [74], the polarization of environment [75], the cavity depth [76], the cavity size and the energy of hydrogen bonds [77], and the interaction potential between the electron and Coulomb or dipole charges of liquid particles [78, 79].

4. Variational evaluation of the effective functional

4.1 Estimation by a trial action

The path integral $\int D[\mathbf{r}] \exp[-S_0]$ can be analytically calculated only for a special form of action S_0 , for example, when this action is the quadratic functional

$$S_0(\mathbf{r}) = \int_0^\beta \left[\frac{m}{2} \dot{\mathbf{r}}^2(\tau) - \frac{1}{\beta^2} \int_0^\beta \alpha(\tau - \tau') |\mathbf{r}(\tau) - \mathbf{r}(\tau')|^2 \right] d\tau d\tau'. \quad (16)$$

In the general case, we can form a variational estimate of the integral, using a quadratic trial action S_0 depending on parameters α [80]. Then one obtains

$$Z \geq Z_0 \exp[\langle S_0(\alpha) - S_{\text{eff}} \rangle_{S_0}],$$

where symbol $\langle \dots \rangle_{S_0}$ denotes averaging with respect to the trial action S_0 , namely,

$$\langle S_0 - S_{\text{eff}} \rangle_{S_0} \equiv \int (S_0 - S_{\text{eff}}) \exp(-S_0) D[\mathbf{r}].$$

The estimate (16) will be optimal, if its right-hand part is maximum:

$$Z \simeq Z_{\text{opt}} \equiv \exp[-\beta F], \quad \frac{\delta F}{\delta \alpha} = 0. \quad (17)$$

As a result, relation (16) yields a set of nonlinear algebraic equations linking the parameters

$$\alpha_m = \int_0^\beta \alpha(\tau) \exp[2i\pi m \beta^{-1} \tau] d\tau$$

of the trial action S_0 and the parameters of the effective functional F_{eff} . For instance, using approximation (3) we derive a nonlinear algebraic equation for the parameter α :

$$3\alpha = \frac{\rho}{\beta} \left\langle (1 + \rho h_{\text{ss}} * f) * \frac{\delta f}{\delta \alpha} \right\rangle = \Pi(\alpha). \quad (18)$$

To solve it, we should find the dependence $f(\alpha)$. In Ref. [58], this was obtained for the case of a simple polarized liquid. Figure 7 plots a graphical solution for the extremum of the free energy functional $F'(\alpha)$ of a solvated electron for various polarizabilities μ of solvent atoms [58]. Curves 1–4 correspond to $\Pi(\alpha)$: 1 — $\mu = 23a_0^3$, 2 — $\mu = 15a_0^3$, 3 — $\mu = 0$, 4 — $\mu = 5a_0^3$ (where a_0 is the Bohr radius); curve 5 applies to $T'(\alpha) = 3\alpha$. As is seen, there exist two solutions for which $F'(\alpha) < 0$: the trivial one ($\alpha = 0$) corresponding to the extended state, and the nontrivial one to the localized electron state.

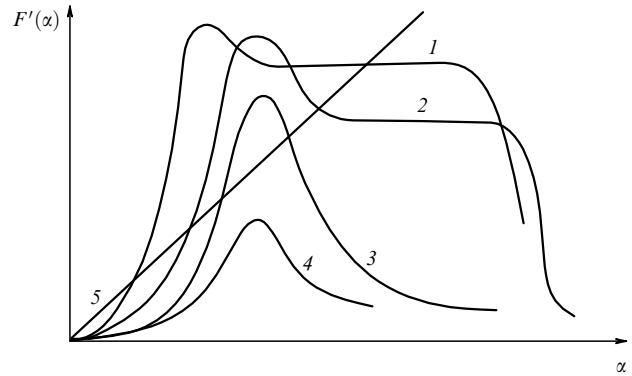


Figure 7. Graphical solution for the extremum of the free energy functional $F'(\alpha)$ of an electron solvated in a simple liquid for various polarizabilities μ of solvent atoms [58]. Curves 1–4 correspond to $\Pi(\alpha)$: 1 — $\mu = 23a_0^3$, 2 — $\mu = 15a_0^3$, 3 — $\mu = 0$, 4 — $\mu = 5a_0^3$ (where a_0 is the Bohr radius); curve 5 represents $T'(\alpha) = 3\alpha$.

The estimate through the trial action (16) was first submitted in the polaron problem [80] for two parameters α_1 and α_2 . A similar method was first applied to a solvated electron in the RISM-polaron model [34], where relations for α_m were derived, the number m of the Fourier transform components approaching several hundred. The advantage of the method considered is that the free energy can be estimated for both the localized and extended electron states. However, a large set of nonlinear algebraic equations should be numerically solved in this case.

4.2 The Schrödinger equation and the effective potential for a solvated electron

On the whole, the trial action method reduces the problem to the calculation of averages and optimization of the estimates.

There is another method for localized electron states, which is similar to the saddle point approach. In this method, a density matrix $\varrho_0(\mathbf{r}, \mathbf{r}')$ is introduced, specifying the trial action S_0 . The optimization of the free energy results in a nonlinear differential equation for $\varrho_0(\mathbf{r}, \mathbf{r}')$. When the electron ground state is not degenerate and therefore $\varrho_0(\mathbf{r}, \mathbf{r}) \sim \varphi^2(r)$, we obtain the nonlinear Schrödinger equation for the wave function of the ground state [58]:

$$\left[-\frac{1}{2} \Delta + V_{\text{eff}}(\{\varphi\}, \mathbf{r}) - E \right] \varphi(\mathbf{r}) = 0, \quad (19)$$

$$V_{\text{eff}}(\{\varphi\}, \mathbf{r}) = -\frac{\rho}{\beta} \left\langle (1 + \rho h_{\text{ss}} * f) \frac{\delta f}{\delta \varphi^2} \right\rangle,$$

where E is the electron energy. Hereinafter we will drop the subscript S_0 in performing the averaging.

The effective potential $V_{\text{eff}}(r)$ is related to the electron–solvent distribution function $g_{\text{es}}(\mathbf{r})$ as

$$V_{\text{eff}}(\mathbf{r}) = \rho g_{\text{es}} * u = \rho \int g_{\text{es}}(\mathbf{r}') u(\mathbf{r} - \mathbf{r}') d\mathbf{r}'. \quad (20)$$

In the modified mean-field theory [49, 50], the Ornstein–Zernike equations are used as an alternative to the RISM-polaron equation. There the typical size α^{-1} of the electron state is considered as a parameter which, in turn, is found from the Schrödinger equation with the potential $V_{\text{eff}}(\mathbf{r})$ depending on $g_{\text{es}}(\mathbf{r})$. The equations are solved using a self-consistent procedure.

A detailed study of the solvated electron behaviour in various liquids essentially depends on the type of liquid, which is determined by the potential $u(\mathbf{r})$. In the general case, the potential $u(\mathbf{r})$ includes short-range [$u(r) = u_0, r < r_0$] and long-range [$u(r) = u_1(r), r > r_0$] parts. Typical behaviour of the potential $u(r)$ is depicted in Fig. 8.

Figure 9 shows the effective potential $V_{\text{eff}}(\mathbf{r})$. It is seen that as a result of redistribution of solvent particles the potentials $V_{\text{eff}}(\mathbf{r})$ and $u(\mathbf{r})$ differ significantly. The effective potential $V_{\text{eff}}(\mathbf{r})$ also includes short-range [$V_s(r) = \rho g_{\text{es}} * u_s$] and long-range [$V_{\text{pol}}(r) = \rho g_{\text{es}} * u_1$] portions (Fig. 9, curves 2 and 3, respectively). The asymptotic behaviour of the effective potential was studied in Ref. [52]. The short-range and long-range parts of the potential coincide with the results of semicontinual theory for a solvated electron [3]. In particu-

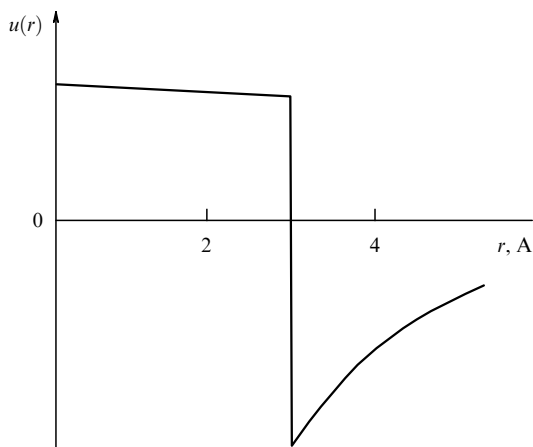


Figure 8. Typical electron–particle pseudopotential $u(r)$.

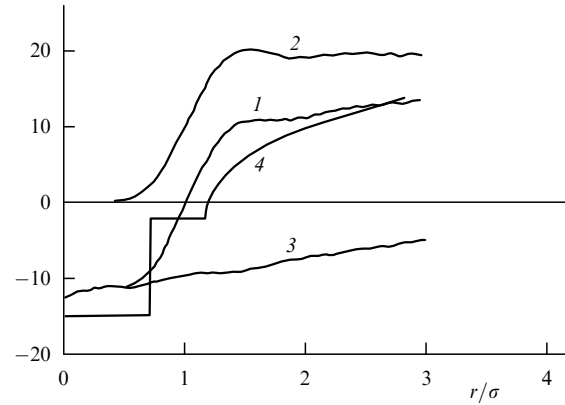


Figure 9. Effective potential $\tilde{V}_{\text{eff}}(\tilde{r}) = 2V_{\text{eff}}(r/\sigma)\sigma^2$ (curve 1) and its short-range $\tilde{V}_s(\tilde{r})$ (2) and long-range $\tilde{V}_{\text{pol}}(\tilde{r})$ (3) portions [50]. Curve 4 corresponds to the semicontinual treatment of $\tilde{V}_{\text{eff}}(\tilde{r})$ [3].

lar, the short-range part is found to be $V_s \sim V_0$, where V_0 is the cavity depth given by solvent parameters. On the other hand, for polar media

$$V_{\text{pol}}(r \rightarrow \infty) \sim -\left(1 - \frac{1}{\epsilon}\right) e^2 \int \varphi^2(\mathbf{R}) |\mathbf{r} - \mathbf{R}|^{-1} d\mathbf{R}$$

(where ϵ is the dielectric constant of the medium).

A mere combination of these two asymptotics effects a semicontinual treatment of the effective potential [3]: a combination of the cavity formation and polaronic tails. In essence, the semicontinual treatment reduces to a piecewise continuous approximation of the effective potential with an arbitrary fitting parameter — the cavity radius. In the statistical approach this parameter is not necessary, and the effective potential can be calculated through microscopic consideration of environment, namely, using the electron–atom interaction pseudopotential $u(\mathbf{r})$ and solvent density correlation functions.

Problems (18) and (19) are much simpler than the straightforward calculation of the partition function (1). They self-consistently determine the dependences $f(\langle u(\mathbf{r}) \rangle)$ or $V_{\text{eff}}(\{g_{\text{es}}, u\})$. From this point of view, the approach considered is one more self-consistent mean-field treatment of the solvated electron.

5. Specific features of the behaviour of a solvated electron in various media

5.1 Simple classical liquids

The behaviour of an excess electron in a simple liquid is determined by two main effects: polarization and short-range interactions between the electron and solvent atoms. In this case the potential $u(r)$ can be approximated as

$$u(r) = u_s(r) \simeq \frac{L}{2} \frac{\delta(r)}{r^2}, \quad r \leq r_0, \\ u(r) = u_1(r) = -\mu e^2 r^{-4}, \quad r \geq r_0. \quad (21)$$

Here $L = 2 \int u_s(r) r^2 dr$ is the scattering length, which can be evaluated experimentally or theoretically [81], $\mu/2$ is the atomic polarizability, and e is the electron charge.

The problem of an excess electron with a short-range interaction potential $u_s(r)$ was probably first examined in Refs [82, 83] by the method of Mayer's functions. Since then it has been considered in a large number of works. Here we outline only the main results related to the polarization effect [58]. At $L \geq 0$, the average generalized Mayer function is written as

$$\langle f(r) \rangle = \exp[-\beta w_s](1 - \beta u_1 * \varphi^2) - 1, \quad w_s(r) = 2\pi L \varphi^2(r). \quad (22)$$

This formula describes the asymptotic behaviour of $\langle f(r) \rangle$ as $r \rightarrow 0$ and $r \rightarrow \infty$. Using this estimate of $\langle f(r) \rangle$, we can find expressions for the short-range (V_s) and long-range (V_{pol}) components of the effective potential and the electron-solvent distribution function g_{es} :

$$V_s = \rho(1 + \rho h_{ss} * f_s) \exp[-\beta w_s] 2\pi L(1 - \beta u_1),$$

$$V_{\text{pol}}(r) = \rho(1 + \rho h_{ss} * f_s) \exp[-\beta w_s] * u_1, \quad (23)$$

$$g_{\text{es}}(r) = (1 + \rho h_{ss} * f_s) \exp[-\beta w_s](1 - \beta u_1 * \varphi^2),$$

$$f_s = \exp[-\beta \omega_s] - 1. \quad (24)$$

In the case of the polarizable medium, the effective potential V_{eff} includes a shift of the potential well $V_{\text{pol}}(r \rightarrow 0) \sim -4\pi\rho\mu e^2\alpha$. With regard to the definition of the dielectric constant $4\pi\rho\mu = (1 - 1/\epsilon)$, we find that the medium polarization leads to an additional contribution to the free energy, equal to $-(1 - 1/\epsilon)\alpha e^2$.

Using the stepwise approximation

$$w_s(r) = 2\pi L \varphi^2(0), \quad r < \alpha^{-1}, \quad w_s(r) = 0, \quad r > \alpha^{-1},$$

we can also obtain an analytical expression for the cavity size α_c , similar to (18). Notice that at large enough α the gradient terms $w(r) \simeq w_s(r) + \nabla^2 \tilde{w}_s(r)$ should be taken into account, which is equivalent to consideration of the interphase at $r \simeq \alpha^{-1}$ and the surface energy $E_s \propto \alpha^{-2}$ [15]. Although this correction somewhat changes the asymptotic behaviour of the free energy $F(\alpha \rightarrow \infty)$ and limiting parameters at which the above states exist, it has little effect on the qualitative variation of the quantities under study.

Using the same stepwise approximation for $w_s(r)$, we can set the condition of clusterization:

$$\rho\beta\mu e^2\alpha^4 \geq C_0, \quad (25)$$

where C_0 is a constant of about unity [57]. It is interesting to note that as the polarizability rises, a phase transition similar to the globule-coil transition takes place [60, 61]. The peripheral part of the isomorphic polymer chain extends gradually, the electron density distribution smooths out and localized electron states disappear (see curve 4 in Fig. 7, for which only extended electron states exist). Then the localized electron states arise again (see Fig. 7, curves 1, 2). However, the newly formed localized electron states differ radically from the cavity-type structures (see Fig. 7, curve 3) since in this case the electron localizes at a thickening of gas density and forms a cluster.

Thus, three situations are principally possible in inert gases and polarizable liquids: (1) the electron localized in a cavity, which corresponds to slight polarization and occurs in liquid helium; (2) the extended electron states (low polarization of medium occurs in liquid argon), and (3) the cluster

formation at an excess electron (strong polarization of medium seems to occur in dense xenon). Clusters are experimentally observed in dense xenon gas [84, 86]. Positronium clusters are experimentally detected in dense helium [87, 88] and argon [89] gases.

Similar analytical estimates for $\langle c_{\text{es}}(r) \rangle$ were derived in Ref. [41] on the basis of the RISM-polaron theory, where the transition from the bubble formation to the cluster state was shown to occur through extended electron states.

Comparison of the theoretical expectations obtained on the basis of the RISM-polaron theory [37] with the results of numerical simulation [31] demonstrates that the statistical theory is suited to describe electron states localized in helium and extended electron states in xenon over a wide range of temperature and density, though slightly overestimating the electron localization. In Ref. [38], the RISM-polaron theory was also used to assess the electron mobility in xenon and argon. The authors calculated the diffusion coefficient ($R^2(t \rightarrow \infty) \sim Dt$), which was finally obtained in the form

$$D^{-1} = \left(\frac{\beta}{72\pi^3} \right)^{1/2} \int_0^\infty k^3 \langle c_{\text{es}}^2(k) \rangle \tilde{\chi}_2(k) \exp\left(-\frac{k^2\beta}{8}\right) dk. \quad (27)$$

The comparison of these calculations with the experimental data [84] reveals qualitatively similar dependences of the electron mobility on the gas density (Fig. 10).

Figure 11 displays the comparison between the work function $V_0(\rho)$ [85] and the mean electron energy $E(\rho)$ [38] in argon. As is seen, their behaviour is similar. The nonmonotone dependences of these quantities on gas density are caused by different effects of short-range and long-range interactions. At low densities the attraction is dominant, while at high densities the short-range repulsion makes the main contribution.

In Ref. [90], the RISM-polaron theory was modified to take into consideration the long-range polarization part u_1 . There the HNC closure was used instead of the PY one. The modification allowed the authors to improve the calculated results compared to those in Ref. [37]. According to the calculations, at high densities the correction resulting from

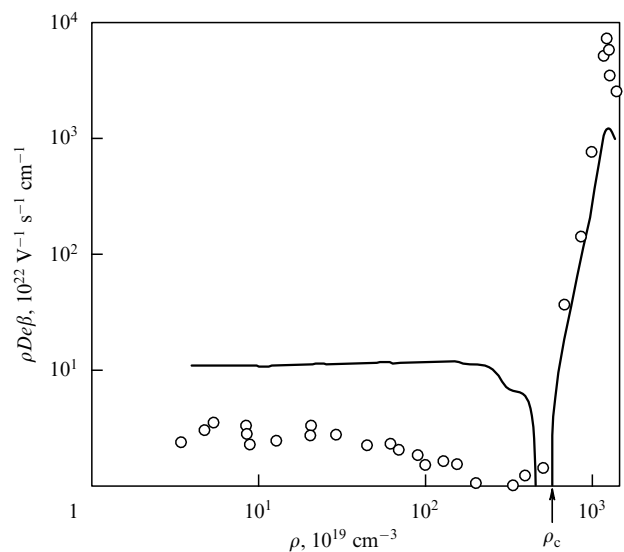


Figure 10. Electron mobility in xenon [38]. The circles correspond to experimental data [84], while the solid line represents calculations using the RISM-polaron theory [38].

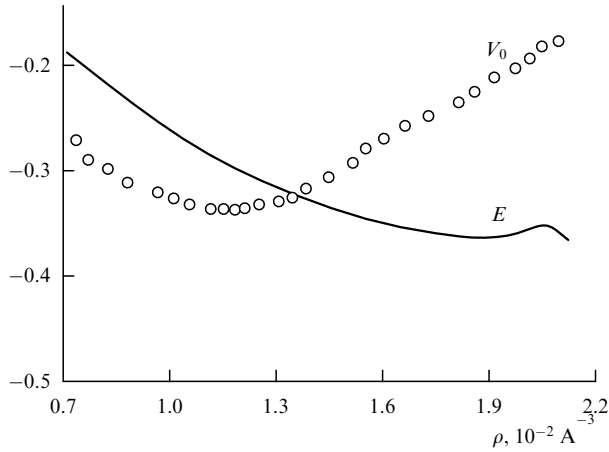


Figure 11. Dependences of the work function V_0 [85] and the mean electron energy E [38] on the solvent density ρ in argon.

the use of different closures is rather small, while at low densities, when the long-range potential is most effective, the HNC closure seems to be more appropriate. However, comparison with the simulation data shows that the RISM-polaron theory is suitable only at high densities, since it does not consider large density fluctuations.

Notice that for inert gases there are also a large number of works using the density functional theory [91–93]. Such treatments constitute a limiting case of the statistical models under review, where only the change in the average density $\langle \rho(r) \rangle$ is taken into account, while the correlations between gas particles are ignored, i.e. $\chi_2 \equiv 0$.

The authors of Ref. [48] revealed that for a solvated electron in a simple classical liquid, when the electron ground state is dominated, the approaches using the direct correlation function and the Mayer function give similar results to the accuracy of terms quadratic in $\langle c_{es}(r) \rangle$.

The authors of Ref. [49] compared calculated results for the electron state localized in a simple classical liquid, obtained by various statistical methods, i.e. those with the estimate of the electron Mayer function $\langle f(r) \rangle$, the direct correlation function $\langle c_{es}(r) \rangle$, and $g_{es}(r)$ computed from the Kirkwood equation (11), with the results of numerical simulation. This comparison revealed that all the cited methods yield rather similar results (Table 1) but the thermodynamic characteristics (electron energy) demonstrate better agreement with the simulation when employing the estimate of $\langle c_{es}(r) \rangle$ with the PY closure. However, the model with the PY closure essentially overestimates the share of the correlation function $g_{es}(r)$, resulting in an anomalously sharp solvate structure around the electron, whereas the other

Table 1. Ground-state electron energy E in a simple classical liquid at $T = 309$ K and various reduced densities $\rho\sigma^3$ [49].

Model†	E , eV			
	$\rho\sigma^3 = 0.9$	0.7	0.5	0.3
Numerical simulation	1.8	1.35	1.08	0.61
Theory				
PY	1.84	1.44	1.08	0.76
WP	1.31	1.14	0.95	0.71
K	1.29	1.12	0.93	0.69

† PY corresponds to the estimate using (9) with the PY closure; WP using (22) for $u_l \equiv 0$, and K using the solution to (11).

models provide results more close to the simulation data. Figure 12 plots the electron–solvent correlation function $g_{es}(r)$ of an electron solvated in liquid helium [49] ($\rho\sigma^3 = 0.9$, $T = 309$ K). Curve 1 fits the estimate obtained from (22) at $u_l \equiv 0$; curves 2 and 3 represent estimates found from (9) with the PY closure and from the solution to (11). The circles represent the simulation data.

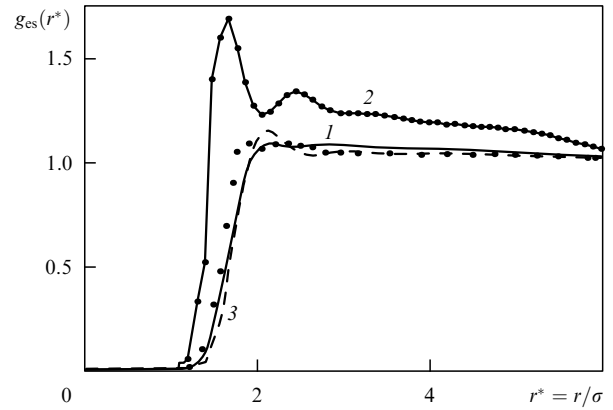


Figure 12. Electron–solvent correlation function $g_{es}(r)$ of an electron solvated in liquid helium [49] ($\rho\sigma^3 = 0.9$, $T = 309$ K). Curve 1 corresponds to the use of (22) at $u_l \equiv 0$, while curves 2 and 3 represent the estimates using (9) with the PY closure and the solution to (11). The circles fit in with the simulation data.

The dependences of the electron effective mass on the parameters of a simple classical liquid (density, temperature, atomic diameter) were calculated in Ref. [43] using the RISM-polaron theory. In the case of the free electron in an external field f , the change in the free energy of the electron is equal to $(24m)^{-1}\beta^3 f^2$. For the solvated electron in a liquid we can define the effective mass m_{eff} in a similar manner, as the coefficient of the second-order correction [43]:

$$\Delta F = (24m_{\text{eff}})^{-1}\beta^3 f^2 + \dots$$

In consequence of this it was shown that as the density rises or temperature decreases the electron passes on from the extended state to the localized one, and the effective mass abruptly increases. Figure 13 plots the dependence of the effective mass $m_{\text{eff}}(\beta^{1/2}/\sigma)$ at various solvent densities [43]. The critical temperature of the transition depends nonmonotonically on the solvent density.

For a simple classical liquid, the authors of Ref. [94] proposed a universal scaling law $R/R_{\text{free}} = Fu(\rho\beta^{1/2}\sigma^2)$, where Fu is a universal function independent of the electron–solvent interaction potential, and σ is the size of the solvent particles. Comparing the computed results obtained with the use of the RISM-polaron theory in these dimensionless variables, they found a minor deviation from the above universal behaviour, the low and upper bounds of the critical density attendant to the electron transition from the extended to the localized state decreasing gradually as $\beta^{1/2}$ increases. This scaling law also allows a correspondence between the data obtained by the statistical methods and those found by numerical simulation for diatomic classical liquids to be set up.

The absorption spectrum of an electron localized in helium was calculated in Ref. [36] and compared with the

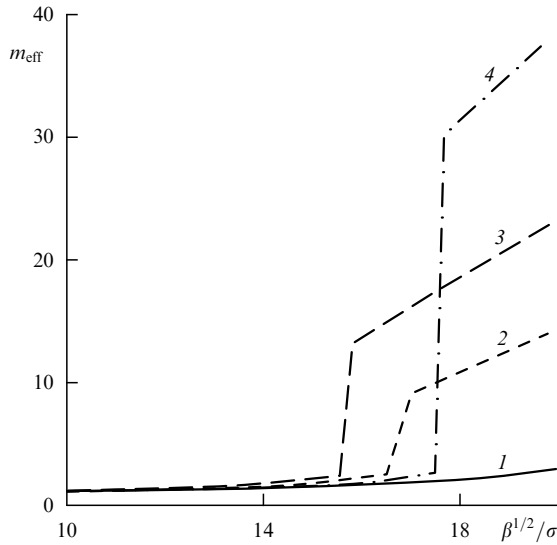


Figure 13. Dependence of the electron effective mass $m_{\text{eff}}(\beta^{1/2}/\sigma)$ for various solvent densities [43]: 1 — $\rho\sigma^3 = 0.3$; 2 — 0.45; 3 — 0.6; 4 — 0.8.

data obtained using Monte Carlo simulation for a quantum particle in helium [95]. Though there is some discrepancy in the results, on the whole, these approaches provide rather similar findings.

The localization and annihilation of positronium in xenon was investigated in Ref. [96] using the RISM-polaron theory and a primitive model with a short-range repulsive potential. This primitive model accords very well with the quantum molecular dynamics data [97]. The decay rate of ortho-positronium, obtained by the theory, correlates fairly well with the results of numerical simulation.

5.2 Polar liquids

In the case of polar liquids the interaction between an excess electron and a solvent particle includes a dipolar attraction proportional to the dipole moment \mathbf{m} of the particle:

$$u_l(\mathbf{r}) = (\mathbf{m}\mathbf{s})u_d(r) = -\frac{\mathbf{m}\mathbf{s}e^2}{r^2}, \quad r > r_0, \quad (27)$$

where \mathbf{s} is the unit vector: $\mathbf{s} = \mathbf{r}/|\mathbf{r}|$. Here the main difference from simple liquids is that the potential $u(\mathbf{r})$ is not spherically symmetric but also depends on angular variables. However, the above consideration can be applied to this potential too, if we separate out terms with different symmetry.

In the general case the electron wave function $\varphi(r)$ is not spherically symmetric either:

$$\varphi(\mathbf{r}) = \varphi_0(r) + \gamma\varphi(r)\mathbf{sm} + \dots$$

However, if the interaction potential is small compared to the lowest excitation energy:

$$\left| \int u_l(\mathbf{r})\varphi_0(r)\varphi_1(\mathbf{r})d\mathbf{r} \right| \ll |E_0 - E_1|,$$

where φ_1 and E_1 are the wave function and the energy of the first excited state with p -symmetry, respectively, we can treat the nonspherical part of the wave function as a small correction ($\gamma \ll 1$) and take it into account using perturbation theory. In the zero-order approximation $\varphi(\mathbf{r}) \approx \varphi_0(r)$ and we can retain only the terms with spherical symmetry.

The terms with different symmetry should also be separated out in the correlation function $h_{ss}(\mathbf{r})$:

$$h_{ss}(\mathbf{r}) = h_s(r) + h_\Delta(r)\Delta + h_D(r)\mathbf{D},$$

$$\Delta(r, s_1, s_2) = (\mathbf{s}_1\mathbf{s}_2), \quad \mathbf{D}(r, s_1, s_2) = 3(\mathbf{s}_1\mathbf{r}_{12})(\mathbf{s}_2\mathbf{r}_{12}) - \Delta,$$

where \mathbf{r}_{12} is the radius vector connecting points 1 and 2.

The analysis suggests that in order to estimate $\langle f(\mathbf{r}) \rangle$ we should take into account the terms proportional to u_d^2 . Then

$$V_{\text{pol}} = \frac{y}{4\pi} \left[1 + \frac{\rho}{3}(h_\Delta + 2h_D) \right] * u_d * \exp[-\beta w_s]u_d, \quad (28)$$

where $y = (4/3)\pi\rho\beta\mathbf{m}^2$. It can be shown that as $r \rightarrow \infty$, $V_{\text{pol}} \rightarrow (4/3)\pi\rho\beta\mathbf{m}^2(1 + \rho h_\Delta^0/3)e^2r^{-1} \approx yg_K e^2r^{-1}$, where $g_K = 1 + (4/3)\pi\rho \int h_\Delta(r)r^2dr$ is the Kirkwood factor. For weakly polar liquids $yg_K \approx 1 - 1/\epsilon$, and we arrive at the result similar to the case of a polarizable liquid with $\mu = \beta\mathbf{m}^2/3$. Analogous relations can be derived for the electron–solvent correlation function $g_{es}(\mathbf{r})$, too. It is not spherically symmetric:

$$g_{es}(\mathbf{r}) = (1 + \rho h_{ss} * f_s) \exp[-\beta w_s](1 - \mathbf{m}\mathbf{s}u_d). \quad (29)$$

We can find an analytical solution for the typical electron size:

$$3\alpha = \frac{4\pi C(\alpha)\rho}{\beta\alpha^4} (1 - \rho h_s^0)(1 - \exp[-3\beta\alpha^3 L]) + \left(1 - \frac{1}{\epsilon}\right) \frac{e^2}{\sqrt{\pi}} c_1, \quad (30)$$

where $c_1(\alpha)$ is a numerical factor ≈ 1.4 for $\sigma\alpha \approx 1$. According to the estimate $a_0\alpha_c \approx (1/3)\sqrt{\pi}a(1 - 1/\epsilon)$ and $\langle R^2 \rangle^{1/2} \approx 2.5$ Å. In most polar liquids the value of $\langle R^2 \rangle^{1/2}$ lies in the range 2–3 Å, i.e. our estimate is close to the experimental data [3]. However, if we evaluate the energetic characteristics of a solvated electron in the above way, we overestimate them. In principle, for actual liquids we should also take into account the terms of higher order in $\langle u_d \rangle$. In this case, an analytical expression of the type of Eqn (30) cannot be derived, but the evaluation of V_{pol} can be performed in the conditions of dominant orientational ordering. Such a potential for an electron solvated in a dipolar liquid was first obtained in Ref. [98] and was recently considered in Ref. [79]. Its main difference from (30) is in that the orientational saturation for this potential occurs at $r \sim \alpha^{-1}$, so V_{pol} is no longer proportional to \mathbf{m}^2 . Figure 9 plots the effective potential $\tilde{V}_{\text{eff}}(\tilde{r}) = 2V_{\text{eff}}(r/\sigma)\sigma^2$ for an electron solvated in a Stockmayer liquid [50].

We assumed in the foregoing that the electron ground state is spherically symmetric, and the asymmetric component of the potential results in a small correction $\delta E_0 \sim (\varphi_0 * u\varphi_1)^2/|E_0 - E_1|$. As u_d increases and $E_0 \rightarrow E_1$, the state will degenerate. In this case the electron ground state should be considered as a combination of $s \pm p$ states. At $E_0 \rightarrow E_1$, the states collapse and the symmetry of the wave function changes. This effect seems to be revealed in Ref. [39] for a hydrated electron, where the calculations were performed at various cut-off radii of the electron–hydrogen potential.

The authors of Ref. [39] used the RISM-polaron theory to describe the behaviour of a hydrated electron. Liquid was modelled with the data on the structural factor of water, found by numerical simulation. According to these calcula-

Table 2. Energy properties of a hydrated electron.

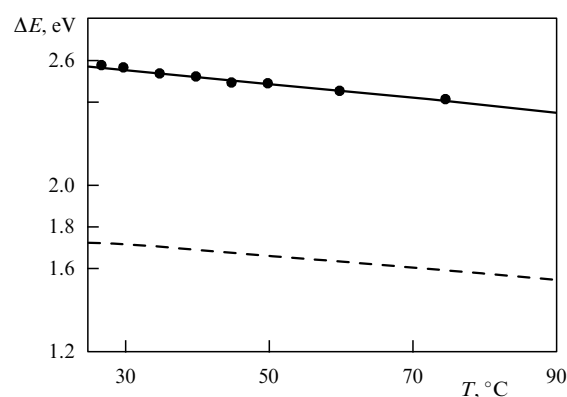
Model	ΔF	ΔE	$-\mathrm{d}\Delta E/\mathrm{d}T$	$\langle T \rangle$	$-\langle \Pi \rangle$	$-E$	$\langle r^2 \rangle^{1/2}$
Numerical simulation							
SPC water model [50]				1.9	4.3	2.4	2.3
Modified SPC water model [50]				1.8	3.6	1.8	2.4
[27]		2.2		2.1		3.0	2.4
Theory							
[50]				1.8	3.6	1.8	2.2
[102]						2.0	2.3
[51]	-0.96	2.6	0.0035	1.82	6.08	4.26	2.0
[39]	-1.62			2.0	7.0–8.0	5.0	2.0
Experiment [7]	-1.61	1.73	0.0029			3.0 [126]	2.1–2.8

tions, both energetic and structural characteristics of the hydrated electron are in good agreement with the results of numerical simulation [26]. The calculated chemical potential of the hydrated electron differs from the experimental one only by 1%. It is interesting to note that as the cut-off radius of the electron–hydrogen potential substantially rises, the electron state becomes supertrapped on hydrogen atoms, which may be related to the above-indicated change in the symmetry of the wave function. Similar calculations with the use of the RISM-polaron theory were carried out at temperatures varying from 25 to 90 °C [51]. In contrast to the previous work, the structure of water was calculated using the extended RISM theory. This allowed the authors to obtain a nonmonotone temperature-dependent isothermal compressibility of water quite close to the experimental dependence. Calculations of various energetic and structural properties of the hydrated electron were also performed and, in particular, the temperature dependence of the excitation energy was presented. The calculated mean square of the electron radius proved to be close to the results of numerical simulation [26].

Table 2 presents the energetic characteristics of the hydrated electron: the chemical potential (F), the energy (E), the average kinetic ($\langle T \rangle$) and potential ($\langle \Pi \rangle$) energies, $\Delta E = E_1 - E_0$, and the mean radius. These values were also calculated by numerical simulation with the use of the simple point charge (SPC) model and the modified SPC model of water [50] or using a statistical treatment [39, 50, 51, 102]. For comparison, Table 2 also lists the relevant experimental data. The calculated electron binding and excitation energies differ from the experimental ones by 30%. However, the temperature dependence of the lowest excitation energy nearly coincides with the results of measurements. Figure 14 plots this dependence for a hydrated electron [51]. The dashed line corresponds to the experimental data.

The influence of temperature, pressure and the concentration of additional ions on the shape of the spectrum was investigated in Ref. [52] with a statistical treatment. The calculated dependences of the absorption maximum on pressure and temperature agree with the experimental evidence [99–101].

An extended version of the polaron approach was studied in Ref. [102] as applied to an electron solvated in a polar liquid. In addition to electron solvation by classical particles this model also took account of the electronic polarization of medium. The polarization was determined using the high-frequency dielectric constant ϵ_∞ , while the state of the solvated electron was approximated by a spherically symmetric distribution, whose mean radius was found by

**Figure 14.** Temperature dependence of the lowest excitation energy ΔE for a hydrated electron [51]. The dashed line corresponds to the experimental data.

extremizing the free energy functional. The latter involved corrections caused by the finite sizes of solvent molecules and the electron state. The solvent molecules were considered as polarizable rigid spheres, while the interaction between an electron and a molecule was treated using the mean spherical approximation. The calculated electron radius and energy agree with those found by the RISM-polaron theory or by the path-integral simulation. Inclusion of the surface energy and the external pressure effects into consideration does not substantially affect the results. The authors concluded that with increasing molecular diameter the electron radius also increases and the electron energy decreases, and the reverse when the polarity (ϵ_0) increases. With decreasing polarizability (ϵ_∞), the electron radius and energy rise.

The authors of Ref. [50] investigated an excess electron solvated in a Stockmayer liquid using the mean-field theory. In contrast to the RISM-polaron treatment where $c_{\text{es}}(r)$ is calculated, the authors evaluated $g_{\text{es}}(r)$ using the Ornstein–Zernike integral equations which involved the mean square of the electron radius. The latter was self-consistently determined via the Schrödinger equation depending on $g_{\text{es}}(r)$. The calculated data on the electron localization, energy properties, and the solvate structure around the electron are close to the results of numerical simulation (see Table 2). According to the computations, the presence of the long-range attraction between the electron and a solvent molecule makes the value of the total electron energy negative in contrast to the case of a nonpolar liquid. This also somewhat reduces the mean electron radius, but the calculated decrease in the radius is less than that obtained in simulations.

An excess electron in a Stockmayer liquid has recently been investigated by path-integral simulation [103]. The results obtained agree with the previous theoretical expectations. According to the computations, the electron localization is mainly determined by the short-range repulsive force between the electron and a solvent molecule. The increase in the dipole moment of a solvent particle enhances the process of electron localization, and decreases the electron ground energy.

5.3 Coulomb systems

An important property of Coulomb systems is the presence of two types of charges. The electron–ion interaction features a short-range electron–cation attraction u_{s+} , which may result in electron localization on the atom.

Calculations for an electron solvated in molten KCl were carried out in Ref. [44] on the basis of the RISM-polaron theory. There the HNC closure was used. The structural factor was taken from the data on the numerical simulation of KCl melt. As a result, the typical electron size was found to be $R \simeq 3.2$ Å at $T = 1000^\circ\text{C}$, and the electron was found to localize on a potassium atom (see Fig. 5 depicting the binary radial distribution function $g_{eK^+}(r)$ in molten KCl [44]). The calculated distribution function $g_{eK^+}(r)$ is close to that found using the path-integral simulation [22]. The authors of Ref. [44] concluded that the difference between these functions at $r \rightarrow 0$ relates to overestimation of the electron localization by the variational method. In Ref. [45], the RISM-polaron model was used to calculate the frequency dependence of the generalized susceptibility and the absorption coefficient $K(\omega)$:

$$K(\omega) \sim \text{Im} \left[i(1 + \exp[-\beta\omega]) \int_{-\infty}^{\infty} dt \exp[i\omega t] \frac{d^2}{2dt^2} R^2(t) \right]. \quad (31)$$

The author found the maximum (ω_{\max}) and the half-width ($\delta\omega$) of the absorption spectrum of the solvated electron to be: $\omega_{\max} \simeq 2.2$ eV and $\delta\omega \simeq 0.6$ eV. The path-integral simulation yields $\omega_{\max} \simeq 1.7$ – 1.8 eV, $\delta\omega \simeq 0.5$ eV, while the experimental finding is $\omega_{\max} \simeq 1.3$ eV. In our opinion, this discrepancy is probably caused by the neglect of the quantum degrees of freedom for liquid (electron–electron interactions). An attempt to improve the results by varying the cut-off radius of the electron–cation pseudopotential [46] insufficiently decreased the variational estimate of the absorption maximum. The inclusion of the rigid-sphere repulsion in the electron–ion potential and variation of the rigid-sphere sizes of ions did not yield a pronounced effect either [47].

The authors of Refs [104, 108] considered the problem of an excess electron in an electrolyte on the basis of the polaron approach. Using functional integration, they wrote the grand partition function as

$$\begin{aligned} \Xi &= \int D[\psi] \exp[-\beta F(\psi, \langle u \rangle)], \\ F(\psi, \langle u \rangle) &= T + \int \left[\nabla \langle u \rangle \nabla \psi - \frac{(\nabla \langle u \rangle)^2}{2\epsilon_\infty} - \frac{(\nabla \psi)^2}{2} \right] d\mathbf{r} \\ &\quad - \rho \beta^{-1} * [f(e\beta\psi) + f(-e\beta\psi)], \end{aligned} \quad (32)$$

where T is the electron kinetic energy, $\langle u \rangle = \int e\phi^2(\mathbf{r})|\mathbf{r} - \mathbf{R}|^{-1} d\mathbf{r}$ is the electron–ion potential, ψ is the total potential of the field induced by all charges, and ϵ_∞ is the high-frequency polarizability caused by electron polarization.

Varying the functional $F(\psi, \langle u \rangle)$, they derived the Schrödinger equation with the potential $V_{\text{eff}}(z) = e[\epsilon_\infty^{-1}\langle u \rangle - \psi]$, where the field potential $\psi(r)$ satisfies the Poisson–Boltzmann equation

$$\Delta\psi = -4\pi e \left(\rho [f(-\beta e\psi) - f(\beta e\psi)] + \varphi^2 \right). \quad (33)$$

In this form the model is yet another application of the statistical treatment, where short-range correlations between ions of the second-order and higher are ignored, while the electron–electron interactions are considered as in the conventional polaron theory [127]. The calculated data on the dependence of the absorption maximum on the ion concentration agree qualitatively with the experimental results, according to which a blue shift is observed as the ion concentration increases [101]. Figure 15 plots the changes in the absorption maximum for the hydrated electron versus the extent of LiCl dissolution [105].

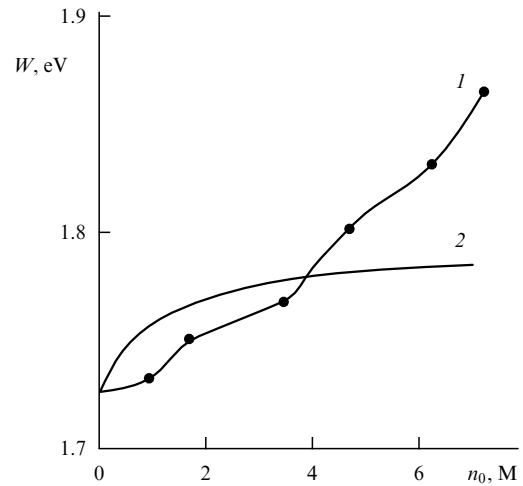


Figure 15. Changes in the absorption maximum for a hydrated electron versus the extent of LiCl dissolution [105]: 1 — experiment, 2 — theory.

6. Many-particle quantum effects

6.1 Electron–electron correlations

The consideration of quantum degrees of freedom of a solvent particle substantially enhances the multiplicity of integral (1), therefore, electron–electron interactions can hardly be taken into account in full measure. One of the simplest approximations permits the Drude model for quantum oscillations of a solvent particle to be used, according to which the dipole moment of a solvent particle $\mu(t)$ fluctuates at a certain frequency ω_0 , i.e. $\mu(t) = \mu_0 \exp(i\omega_0 t)$. For such a liquid the correlation functions $h_{ss}(r, \mu_0, \omega_0)$ can be calculated numerically using the mean spherical approximation [110, 111]. The electronic properties (spectrum of electronic excitations) for such a polarizable liquid with internal degrees of freedom have been intensively investigated [110–116]. Without making a detailed comparison of the cited works, we only indicate that all they actually reduce the problem to the evaluation of a correlation function $h_{\text{eff}}(r)$ for a classical liquid with an effective interaction potential. Having written the long-range part of the electron–atom pseudopotential for the liquid as $u_l(\mathbf{r} - \mathbf{r}(t), t) = -\mu(t)\mathbf{r}\mathbf{r}^{-3}$, one can calculate

$h_{\text{eff}}(r, \mu_0, \omega_0)$. Then the derived expression is substituted into the above formulae and the influence of quantum oscillations of electronic shells on the solvated electron is taken into account.

Calculations of this type were performed using the RISM-polaron theory [37]. Figure 16 shows the calculated changes in the free energy $\beta\Delta F$ versus the reduced solvent density $\rho\sigma^3$ for various polarizabilities μ and reduced frequencies $\bar{\omega} = \omega_0\sigma^2$. Notice that the case $\bar{\omega} \rightarrow 0$ corresponds to a classical polarizable liquid, while $\bar{\omega} \rightarrow \infty$ corresponds to the adiabatic approximation. As is seen from the figure, the inclusion of quantum corrections can substantially (many-fold) change the solvated electron energy.

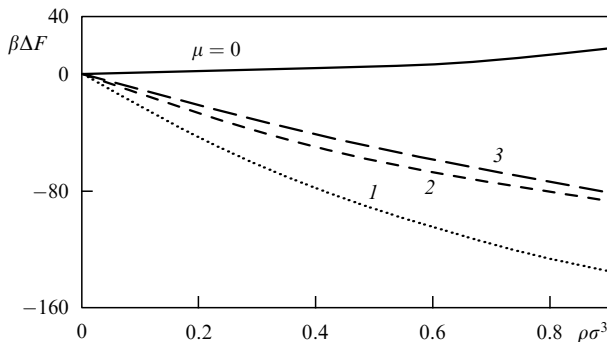


Figure 16. Reduced free energy $\beta\Delta F$ of an electron solvated in a polarizable liquid versus the reduced solvent density $\rho\sigma^3$ for various polarizabilities μ and reduced frequencies $\bar{\omega}$ [37]: 1–3 — $\mu = 0.1\sigma^3$; 1 — $\bar{\omega} = 0.1$; 2 — $\bar{\omega} = 1$; 3 — $\bar{\omega} = 10$.

6.2 The problem of a dielectron

The significance of taking into account the electron–electron interaction is especially conspicuous in the problem of a dielectron (bipolaron), i.e. two excess electrons solvated in a liquid and forming a coupled state. This problem seems to have been first considered in detail for a number of liquids (water, ammonium) and polar matrices (ice, triethylamine, etc.) on the basis of the semicontinual approximation [117]. The authors showed that in all the cited media, the dielectron states are stable and energetically preferable to two single-electron states. No experimental data to confirm these conclusions have yet been obtained. Numerical simulations using quantum molecular dynamics yield different results for water [118] and metal–ammonium solutions [119]. According to the computer simulations, dielectron states are stable in water, while in a metal–ammonium solution only the singlet spin-pairing states of dielectron are stable, the triplet one decaying at a metal concentration of about 1 mol%. The pronounced effect of spin-pairing states was observed in the experiment [120, 121] as a sharp decrease of magnetic susceptibility (Fig. 17). Numerical calculations [122] using quantum molecular dynamics and the Kohn–Sham method demonstrate that the bipolarons form a cluster, and the electrons become delocalized as the metal concentration further increases. A similar transition was also revealed for fermions solvated in a rigid-sphere classical liquid [123].

A statistical model of a dielectron was considered in Ref. [55] by the method of generalized Mayer functions. There the free energy functional and the effective potential for the dielectron and their asymptotic behaviour were considered, ignoring electron–electron correlations. It

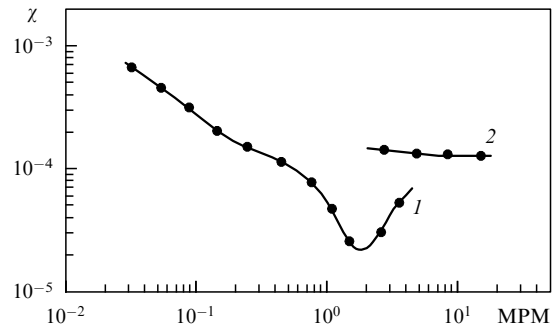


Figure 17. Experimental dependence of the paramagnetic susceptibility χ in metal–ammonium solution on the metal concentration [121]: curve 1 corresponds to $T \approx 240$ K; curve 2 to $T = 373$ K.

should be reiterated that for actual liquids the electron–electron interaction has to be taken into account, but it is a rather labourious procedure. The numerical calculations of a dielectron performed in Ref. [55] confirm this conclusion, revealing the stability of the dielectron state to be rather sensitive to these interactions. Notice that the necessity of including electron–electron interactions was repeatedly pointed out [117, 119].

7. Scope for the statistical approach

We have reviewed the general relationships determining the behaviour of an electron solvated in a classical liquid. The main criterion for applicability of the statistical method is the condition that the number ΔN of particles bound to the electron and given by (5) be large, i.e. $\Delta N \gg 1$. Note that the opposite limit $\Delta N \rightarrow 0$ corresponds to two electron states: when the electron is strongly bound to a single solvent particle and we should use quantum-chemical calculations for the electron–particle complex, or when the electron is extended over the whole volume and does not form any bound states.

The comparison of the results of theoretical treatment, numerical simulations, and experimental data on an electron solvated in various liquids shows that the statistical theory is rather suited to describe thermodynamic and structural properties of the solvated electron in most cases. The variety of statistical approaches relates mainly to the following factors:

- (1) various approximations of the electron–atom pseudopotential $u(r)$ are used;
- (2) various correlation functions are chosen to describe electron–solvent interactions;
- (3) various closures relating these correlation functions are applied.

The first factor is not essential [46, 47], when it does not lead to a change in the symmetry of the electron state. In view of the quantum behaviour of a solvated electron the third factor does not, generally, result in any qualitative changes either, but it can provide a correction [90]. The second factor is chiefly responsible for the differences in estimates obtained by different statistical methods.

Notice that the use of variational estimates is a conventional procedure; it is similar to the density functional method [91–93], the optimal fluctuation method for electron states in disordered systems [124] and variational estimates in the fluctuation theory [125]. In the general case, the effective functional F_{eff} of the solvated electron can be written as an

infinite asymptotic power series in density ρ . It is difficult to assess whether it is appropriate to restrict the consideration in form (13) or (14) to only a finite number of terms of the series. The method of collective variables [66] could provide a basis for assessments of this type. This method could accelerate the convergence of cluster expansions and restrict the number of the terms accounted for in the free energy functional.

In most models under consideration the liquid is treated as classical. In some situations this leads to overestimation of the energetic and especially kinetic characteristics of the solvated electron. Note that the condition for a liquid to be classical is not so rigid in the statistical model. The way of taking into account quantum effects of the environment was described in Section 6. In the case of ‘soft’ electronic shells, when $\omega \gg E_0$, where ω is a characteristic frequency of the electron shell oscillations, this results in the polaron effect and can be taken into account by the replacement of the factor of $1 - 1/\epsilon$ by the Pekar factor $1/\epsilon_\infty - 1/\epsilon$ in the terms proportional to $\varphi^2 * u * \varphi^2$ [109, 127]. Otherwise, when $\omega \simeq E_0$, the electronic shells weakly affect the electron ground state, however, their influence on the absorption spectrum of the solvated electron can be substantial.

Performing averaging, we actually considered only diagonal elements of the density matrix $\varrho(r, r) \propto \varphi^2(r)$ and ignored the off-diagonal ones. The nondiagonal disorder becomes significant in the case of a dominant short-range attractive potential ($u_s < 0$). Examples of such calculations are presented in Ref. [114].

We have not also considered the effects caused by a finite value of the volume of the system or the number of particles in it. Such effects are important for clusters [128]; in particular, they may result in the formation of surface localized electron states.

The problem of the solvated electron in a liquid near a phase transition point remained beyond the scope of our review. In this case the electron interacting with the fluctuations of the order parameter forms a new fluctuon state. The physics of fluctuons was considered in Ref. [125].

8. Conclusions

In our opinion, the statistical approach considered in the review is a powerful method allowing us to calculate the thermodynamic properties and structural characteristics of the solvated electron on the microscopic level. It enables us to evaluate self-consistently the behaviour of a quantum particle in various media, depending on the molecular structure and thermodynamic state of the medium. The possibility of taking account of many-body quantum effects such as electron polarization and bipolaron formation gives a wide opportunity to extend the method to other problems. The statistical approach combined with the quantum molecular dynamics method can serve to find nonequilibrium characteristics of the solvated electron or to calculate the electron behaviour in complex media (polymer liquids, glasses, etc.). We hope new interesting results will be obtained in this field in the near future.

In conclusion we wish to thank V D Lakhno for a useful discussion and D Thirumalai, D Chandler, R Cukier, G Malescio, J P Hernandez, and B N Miller for presentation of their preprints.

References

- Jortner J, Kestner N R (Eds) *Electrons in Fluids* (Berlin: Springer-Verlag, 1973)
- Kevan L, Webster B C (Eds) *Electron – Solvent and Anion – Solvent Interactions* (Amsterdam: Elsevier, 1976)
- Kevan L, Feng D F *Chem. Rev.* **80** 1 (1980)
- Itskovitch E M, Kuznetsov A M, Ulstrup J, in *The Chemical Physics of Solvation* (Eds R R Dogonadze et al.) (Amsterdam: Elsevier, 1988)
- Ferradini C, Jay-Gerin J-P (Eds) *Excess Electrons in Dielectric Media* (Boca Raton: CRC Press, 1991)
- Pikaev A K *The Solvated Electron in Radiation Chemistry* (Jerusalem: World Univ., 1970)
- Hart E J, Anbar M *The Hydrated Electron* (New York: Wiley-Interscience, 1970) [Translated into Russian (Moscow: Atomizdat, 1973)]
- Tompson J C *Electrons in Liquid Ammonia* (Oxford: Clarendon Press, 1976) [Translated into Russian (Moscow: Mir, 1979)]
- Pikaev A K *Sovremennaya Radiatsionnaya Khimiya: Radioliz Gazov i Zhidkostei* (Contemporary Radiation Chemistry: Radiolysis of Gases and Liquids) (Moscow: Nauka, 1986)
- Pikaev A K *Sovremennaya Radiatsionnaya Khimiya: Tverdoe Telo i Polimery. Prikladnye Aspekty* (Contemporary Radiation Chemistry: Solids and Polymers) (Moscow: Nauka, 1987)
- Khrapak A G, Yakubov I T *Elektrony v Plotnykh Gazakh i Plazme* (Electrons in Dense Gases and Plasma) (Moscow: Nauka, 1981)
- The Study of Fast Processes and Transient Species by Electron Pulse Radiolysis* (NATO Advanced Study Institute Series, Ser. C, Vol. 86; Eds J H Baxendale, F Busi) (Dordrecht: D Reidel Publ. Co., 1982)
- Farhataziz R M A, Rodgers M A J (Eds) *Radiation Chemistry: Principles and Applications* (New York: VCH Publ., 1987)
- Careri G, Fasoli U, Gaeta F S *Nuovo Cimento* **15** 774 (1960)
- Springett B E, Jortner J, Cohen M H *J. Chem. Phys.* **48** 2720 (1968)
- Shikin V B, Monarkha Yu P *Dvumernye Zaryazhennye Sistemy v Gelii* (Two-Dimensional Charged Systems in Helium) (Moscow: Nauka, 1989)
- Golden S, Tuttle T R, Jr. *J. Chem. Soc. Faraday Trans.* **2** 78, 1581 (1982)
- Petrucchi S J. *Mol. Liquids* **54** 173 (1992)
- Schnitker J, Rossky P J *J. Phys. Chem.* **93** 6965 (1989)
- Chandler D, Wolynes P G *J. Chem. Phys.* **74** 4078 (1981)
- Berne B J, Gallicchio E *Absorption Spectrum of an Excess Electron in Water*, in <http://www.mhpc.edu/research/ss95/ssp03.html>
- Parrinello M, Rahman A J. *Chem. Phys.* **80** 860 (1984)
- Bartholomew J, Hall R, Berne B J *Phys. Rev. B* **32** 548 (1985)
- Berne B J, Thirumalai D *Ann. Rev. Phys. Chem.* **37** 401 (1986)
- Wallqvist A, Thirumalai D, Berne B J *J. Chem. Phys.* **85** 1583 (1986)
- Sprink M, Impey R W, Klein M L *J. Stat. Phys.* **43** 967 (1986)
- Schnitker J, Rossky P J *J. Chem. Phys.* **86** 3471 (1987)
- Marchi M, Sprink M, Klein M L *Faraday Discuss. Chem. Soc.* **85** 373 (1988)
- Barnett R N et al. *J. Chem. Phys.* **89** 382 (1989)
- Zhu J, Cukier R I *J. Chem. Phys.* **98** 5679 (1993)
- Coker F, Berne B J, Thirumalai D *J. Chem. Phys.* **86** 5689 (1994)
- Chandler D *Studies in Statistical Mechanics VIII* (Eds E W Montroll, J L Lebowitz) (Amsterdam: North-Holland, 1982)
- Chandler D, Singh Y, Richardson D M *J. Chem. Phys.* **81** 1975 (1984)
- Nichols III A L et al. *J. Chem. Phys.* **81** 5109 (1984)
- Nichols III A L, Chandler D J. *Chem. Phys.* **84** 398 (1986)
- Nichols III A L, Chandler D J. *Chem. Phys.* **87** 6671 (1987)
- Laria D, Chandler D J. *Chem. Phys.* **87** 4088 (1987)
- Hsu D, Chandler D J. *Chem. Phys.* **93** 5075 (1990)
- Laria D, Wu D, Chandler D J. *Chem. Phys.* **95** 4444 (1991)
- Chandler D, Leung K *Ann. Rev. Phys. Chem.* **45** 1500 (1994)
- Leung K, Chandler D *Phys. Rev. E* **49** 2851 (1994)
- Sethia A, Singh Y *Phys. Rev. B* **42** 6090 (1990)
- Sethia A, Singh Y *Phys. Rev. B* **46** 9958 (1992)
- Malescio G, Parrinello M *Phys. Rev. A* **35** 897 (1987)
- Malescio G *Phys. Rev. A* **36** 5847 (1987)
- Malescio G *Mol. Phys.* **69** 895 (1990)
- Malescio G *Nuovo Cimento D* **13** 1031 (1991)

48. Shaw M R, Thirumalai D J. *Chem. Phys.* **93** 3450 (1990)
49. Zhu J, Cukier R I J. *Chem. Phys.* **99** 1288 (1993)
50. Zhu J, Cukier R I J. *Chem. Phys.* **99** 5384 (1993)
51. Miura S, Hirata F J. *Phys. Chem.* **98** 9649 (1994)
52. Chuev G N Zh. *Eksp. Teor. Fiz.* **105** 626 (1994) [*JETP* **78** 334 (1994)]
53. Chuev G N *Perspectives in Polarons* (Eds G N Chuev, V D Lakhno) (Singapore: World Scientific, 1997)
54. Chuev G N Zh. *Fiz. Khim.* **69** 1375 (1995)
55. Chuev G N *Izv. Ross. Akad. Nauk Ser. Fiz.* **59** (8) 95 (1995)
56. Chuev G N *Physica D* **83** 68 (1995)
57. Chuev G N *Izv. Ross. Akad. Nauk Ser. Fiz.* **60** (9) 2 (1996)
58. Chuev G N *Izv. Ross. Akad. Nauk Ser. Fiz.* **61** (9) 1770 (1997)
59. Wiegell F W *Introduction to Path-Integral Methods in Physics and Polymer Science* (Singapore: World Scientific, 1986)
60. Grosberg A Yu, Khokhlov A R *Statisticheskaya Fizika Makromolekul* (Statistical Physics of Macromolecules) (Moscow: Nauka, 1989) [Translated into English (New York: AIP Press, 1994)]
61. Lifshits I M, Grosberg A Yu, Khokhlov A R *Usp. Fiz. Nauk* **127** 353 (1979) [*Sov. Phys. Usp.* **22** 123 (1979)]
62. Ishihara A *Statistical Physics* (New York: Academic Press, 1971) [Translated into Russian (Moscow: Mir, 1973)]
63. Hansen J P, McDonald I R *Theory of Simple Liquids* (London: Academic Press, 1986)
64. Kovalenko N P, Fisher I Z *Usp. Fiz. Nauk* **108** 209 (1972) [*Sov. Phys. Usp.* **15** 592 (1973)]
65. Rowlinson J S, Widom B *Molecular Theory of Capillarity* (Oxford: Clarendon Press, 1982)
66. Yukhnovskii I R, Golovko M F *Statisticheskaya Teoriya Klassicheskikh Ravnovesnykh Sistem* (Statistical Theory of Classical Equilibrium Systems) (Kiev: Naukova Dumka, 1980)
67. Mayer J E J. *Chem. Phys.* **18** 1426 (1950)
68. Anderson P W *Phys. Rev.* **109** 1492 (1958)
69. Mott N F, Davis E A *Electronic Processes in Non-Crystalline Materials* (Oxford: Oxford University Press, 1979) [Translated into Russian (Moscow: Mir, 1982)]
70. Ziman J M *Models of Disorder* (Cambridge: Cambridge University Press, 1979) [Translated into Russian (Moscow: Mir, 1982)]
71. Schnitker J, Rossky P J J. *Chem. Phys.* **86** 3462 (1987)
72. Bachelet G B, Ceperley D M, Chiochetti M G B *Phys. Rev. Lett.* **62** 2088 (1989)
73. Del Buono G S, Rossky P J, Murphrey T H J. *Phys. Chem.* **96** 7761 (1992)
74. Gaathon A, Jortner J, in *Electrons in Fluids* (Eds J Jortner, N R Kestner) (Berlin: Springer-Verlag, 1973)
75. Tachiya M, Tabata Y, Oshima K J. *Phys. Chem.* **77** 263 (1973)
76. Funabashi K, Maruyama Y J. *Chem. Phys.* **55** 4494 (1971)
77. Bartczak W M, Hilczer M, Kroh J J. *Phys. Chem.* **91** 3894 (1987)
78. Hilczer M, Bartczak W M J. *Phys. Chem.* **91** 3834 (1987)
79. Hilczer M, Bartczak W M J. *Phys. Chem.* **97** 508 (1993)
80. Feynman R P *Statistical Mechanics* (Reading, Mass.: Addison-Wesley, 1972) [Translated into Russian (Moscow: Mir, 1975)]
81. Atrazhev V M, Yakubov I T Zh. *Eksp. Teor. Fiz.* **108** 604 (1995) [*JETP* **81** 326 (1995)]
82. Friedberg R, Luttinger J M *Phys. Rev. B* **12** 4460 (1975)
83. Luttinger J M *Phys. Rev. B* **13** 2596 (1976)
84. Huang S-S, Freeman G R J. *Chem. Phys.* **68** 1355 (1978)
85. Reininger R et al. *Phys. Rev. B* **28** 4426 (1983)
86. Dmitrenko V V et al. Zh. *Tekh. Fiz.* **53** 2343 (1983) [*Sov. Phys. Tech. Phys.* **28** 1440 (1983)]
87. Roellig L O, Kelly T M *Phys. Rev. Lett.* **15** 746 (1965)
88. Canter K F, Roellig L O *Phys. Rev. Lett.* **25** 328 (1970)
89. Tuomisaari M, Rytölä K, Hautiojärvi P *Phys. Lett. A* **112** 279 (1985)
90. Chen J, Miller B N J. *Chem. Phys.* **100** 3013 (1994)
91. Khrapak A G, Yakubov I T *Usp. Fiz. Nauk* **129** 45 (1979) [*Sov. Phys. Usp.* **22** 703 (1979)]
92. Miller B N, Reese T *Phys. Rev. A* **39** 4735 (1989)
93. Hernandez J P *Rev. Mod. Phys.* **63** 675 (1991)
94. Cao J, Berne B J J. *Chem. Phys.* **102** 432 (1995)
95. Gallicchio E, Berne B J J. *Chem. Phys.* **101** 9909 (1994)
96. Chen J, Miller B N *Phys. Rev. B* **49** 15615 (1994)
97. Reese T, Miller B N *Phys. Rev. E* **47** 2581 (1993)
98. Iguchi K J. *Chem. Phys.* **48** 1735 (1968)
99. Jou F Y, Freeman G R J. *Phys. Chem.* **81** 909 (1977)
100. Golden S, Tuttle T R, Lwenje S M J. *Phys. Chem.* **91** 1360 (1987)
101. Kreitus I V J. *Phys. Chem.* **89** 1987 (1985)
102. Rips I, Tachiya M J. *Chem. Phys.* **107** 3924 (1997)
103. Graf P, Nitzan A, Diercksen G H F J. *Phys. Chem.* **100** 18916 (1996)
104. Lakhno V D, Vasil'ev O V *Chem. Phys.* **153** 147 (1991)
105. Lakhno V D, Vasil'ev O V *Chem. Phys. Lett.* **177** 147 (1991)
106. Vasil'ev O V, Lakhno V D Zh. *Fiz. Khim.* **65** 2104 (1991)
107. Lakhno V D, Vasil'ev O V *Phys. Lett. A* **152** 300 (1991)
108. Vasil'ev O V "Localized electron states in a medium with movable ions", Thesis for Candidate of Physicomathematical Sciences (Moscow, 1991)
109. Pekar S I *Issledovaniya po Élektronnoï Teorii Kristallov* (Research on Electron Theory in Crystals) (Moscow: Gostekhizdat, 1951) [Translated into English (Washington, U.S.: AEC, 1963)]
110. Chandler D, Schweizer K S, Wolynes P G *Phys. Rev. Lett.* **49** 1100 (1982)
111. Høye J S, Olaussen K J. *Chem. Phys.* **77** 2583 (1982)
112. Schweizer K S, Chandler D J. *Chem. Phys.* **78** 4118 (1983)
113. Logan D E, Winn M D J. *Phys. C* **21** 5773 (1988)
114. Stratt R M *Ann. Rev. Phys. Chem.* **41** 175 (1990)
115. Leegwater J A, Mukamel S *Phys. Rev. A* **49** 146 (1994)
116. Schvaneveldt S J, Loring R F J. *Chem. Phys.* **101** 4133 (1994)
117. Feng D-F, Feuki K, Kevan L J. *Chem. Phys.* **58** 3281 (1973)
118. Kaukonen H-P, Barnett R N, Landman U J. *Chem. Phys.* **97** 1365 (1992)
119. Martyna G J, Deng Z, Klein M L J. *Chem. Phys.* **98** 555 (1993)
120. Nicoloso N, Freyland W J. *Phys. Chem.* **87** 1997 (1987)
121. Nakamura Y J. *Phys. IV* (Suppl.) **1** C5-61 (1991)
122. Deng Z, Martyna G J, Klein M L *Phys. Rev. Lett.* **71** 267 (1993)
123. Alavi A, Frenkel D J. *Chem. Phys.* **97** 9249 (1992)
124. Lifshits I M, Gredeskul S A, Pastur L A *Vvedenie v Teoriyu Neuporyadochennykh Sistem* (Introduction to the Theory of Disordered Systems) (Moscow: Nauka, 1982) [Translated into English (New York: Wiley, 1988)]
125. Krivoglaz M A *Usp. Fiz. Nauk* **111** 617 (1973) [*Phys. Usp.* **16**(6) 856 (1974)]
126. Coe J V et al. *J. Chem. Phys.* **92** 3980 (1990)
127. Lakhno V D, Chuev G N *Usp. Fiz. Nauk* **165** 285 (1995) [*Phys. Usp.* **38** 273 (1995)]
128. Barnett R N et al. *Acc. Chem. Res.* **22** 350 (1990)